Supporting Information:

A Novel Ring-Shaped Phosphovanadomolybdate Built by Bicapped Pseudo-Keggin Clusters and Copper(II) Complexes

Jingyang Niu, Guo Chen, Junwei Zhao, Chunfa Yu, Pengtao Ma, Jingping Wang*

[1]Institute of Molecular and Crystal Engineering, College of Chemistry and Chemical Engineering, Henan University, Kaifeng, Henan 475004,P. R. China; [2]College of Pharmacy, Henan University, Kaifeng, Henan 475004,P. R. China

E-mail: jpwang@henu.edu.cn

I. Experimental section

II. Crystal structure figures

III. Physical measurement and characterization

IV. Cationic exchange property study

I. Experimental Section.

1. Materials and Methods: All chemicals were commercially purchased and used without further purification. The TG analysis was conducted on Mettler-Toledo TGA/SDTA851^e analyzer under the nitrogen gas atmosphere with a heating rate of 10 °C/min from 25 °C to 800 °C. UV spectrum was obtained on a Agilent HP8453 UV-Vis spectrometer (distilled water as solvent) in the range of 400–190 nm. IR spectrum was recorded on a Nicolet FT-IR 360 spectrometer using KBr pellets in the range of 4000–400 cm^{-1}. C, H and N elemental analyses were performed on a Perkin-Elmer 2400-II CHNS/O analyzer. XPS analysis was performed on an AXIS ULTRA spectrometer with an Al Kα achromatic X-ray source. XRPD measurement was performed on a Philips X'Pert-MPD instrument with Cu Kα radiation (λ = 1.54056 Å) in the angular range 2θ = 6–40° at 293 K.

2. The synthesis of compound 2: A mixture of $CuCl_2{\cdot}2H_2O$ (1.200 g, 7.039 mmol), $Na_2MoO_4{\cdot}2H_2O$ (1.600 g, 6.613 mmol), NH_4VO_3 (0.800 g, 6.839 mmol), 1,2-dap (0.600 mL, 7.042 mmol), phen (0.076 g, 0.384 mmol), H_3PO_4 (0.5 mL, 50%) and distilled water (12 mL) at pH 7.0 was stirred for 20 min. The mixture was then transferred to a Teflon-lined stainless steel autoclave (30 mL) and kept at 170 °C for 6 days. After being slowly cooled to room temperature, block-shaped black crystals were isolated (42% based on Mo), then washed with distilled water and air-dried at room temperature.

3. The cell parameter of compound 2: Triclinic system, space group *P*-1 with a = 12.5639(12), b = 18.0617(18), c = 20.306(2) Å; α = 67.512(1), β = 85.134(1), γ = 87.603(1)°.

II. Crystal structure figures.

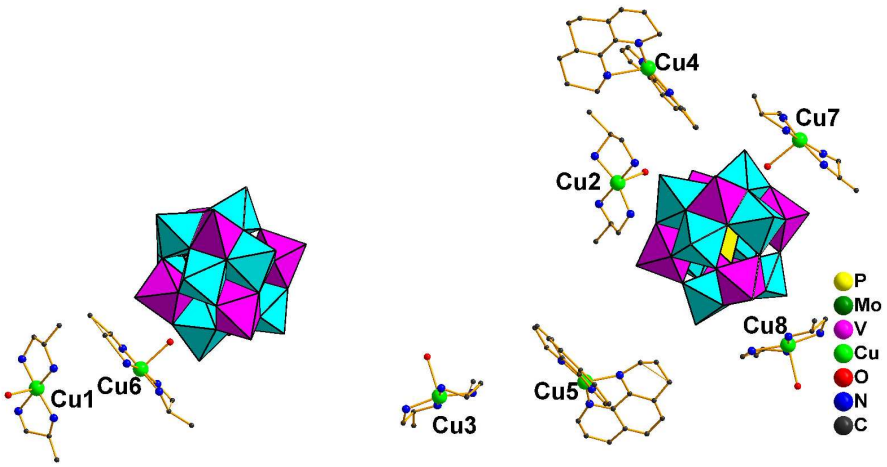

Figure S1 Polyhedral/ball-and-stick view of **2**.

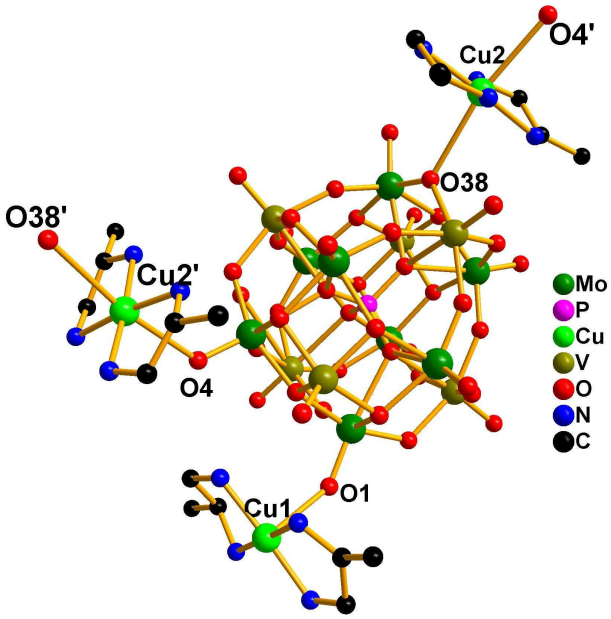

Figure S2 Ball-and-stick view of the cluster $[Cu(1,2\text{-dap})_2\{PMo^{VI}_8V^{IV}_4O_{40}(V^{IV}O)_2Cu(1,2\text{-dap})_2\}]^{3-}$.

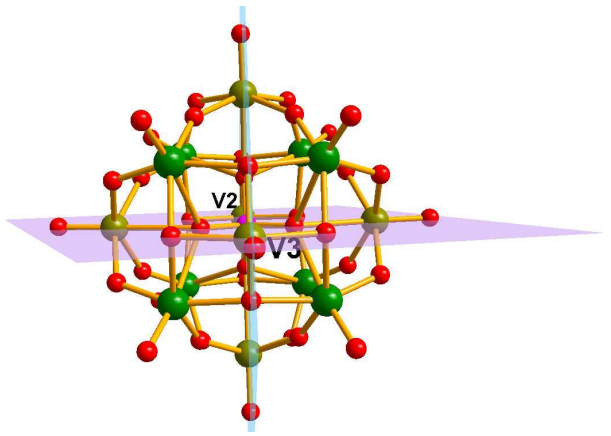

Figure S3 The C_{2V} symmetry of the bicapped pseudo-Keggin structure.

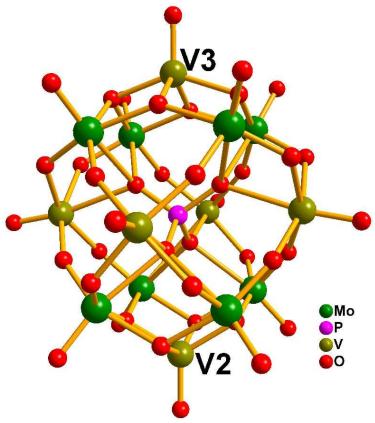

Figure S4 The pseudo-Keggin anion capped by two five-coordinate {VO} units forming the bicapped pseudo-Keggin anion.

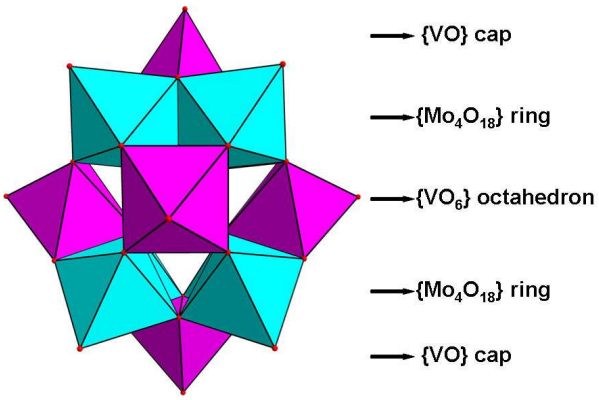

Figure S5 Polyhedral view of the polyoxoanion cluster $[PMo^{VI}_{8}V^{IV}_{4}O_{40}(V^{IV}O)_2]^{7-}$ showing the alternating vanadium and molybdenum oxide layers.

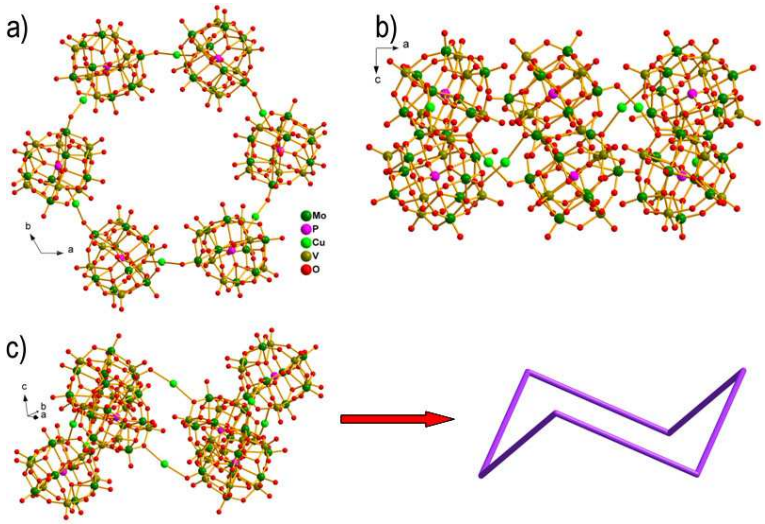

Figure S6 Ball-and-stick view of the ring-shaped cluster **1a**. (a) viewed down the crystallographic *c* axis; (b) viewed down the crystallographic *b* axis; (c) side view: **1a** exhibits the cyclohexane-like ring-shaped structure. (All C, N and Cu1 atom are omitted for clarity)

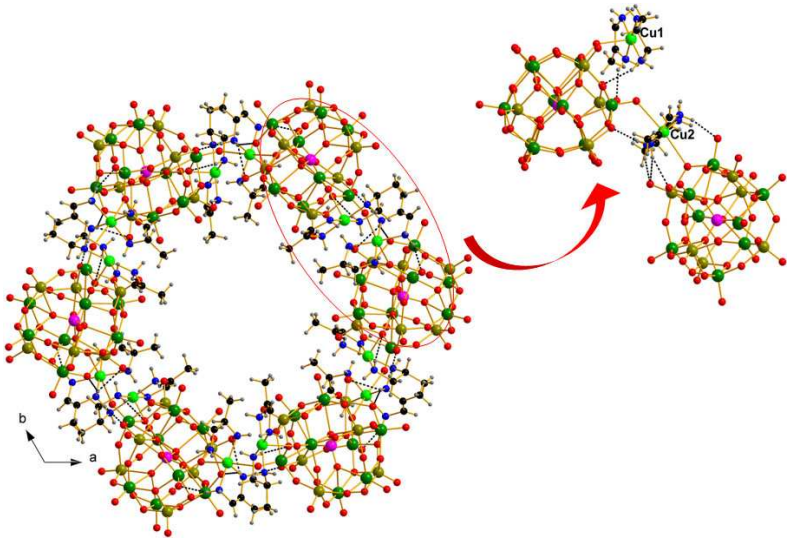

Figure S7 The the N–H•••O hydrogen bonds between $[Cu(1)(1,2\text{-dap})_2]^{2+}$, $[Cu(2)(1,2\text{-dap})_2]^{2+}$ cations and **1b** clusters. Hydrogen bonds are shown as black dotted lines.

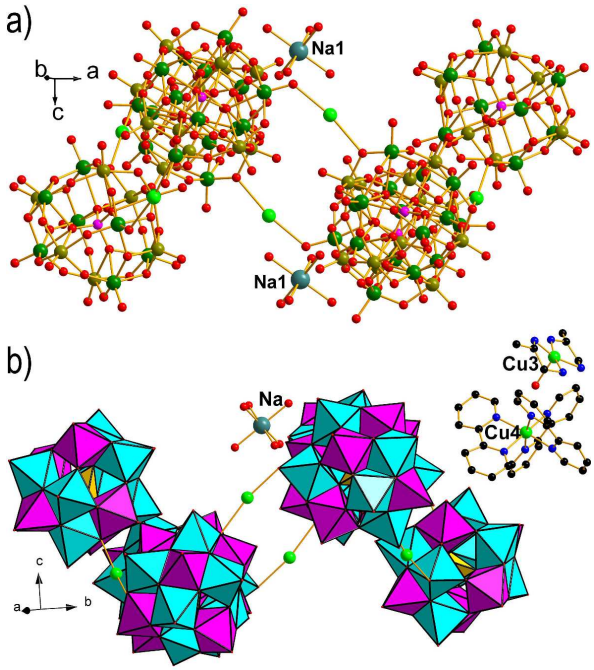

Figure S8 (a) The $\{Na(H_2O)_6\}^+$ ions are along the S_6 symmetry axis of the ring (All C, N and Cu1 atom are omitted for clarity); (b) the isolated countercations, $[Cu(3)(1,2\text{-dap})_2(H_2O)]^{2+}$ and $[Cu(4)(2,2'\text{-bipy})_3]^{2+}$ distribute around the polyoxoanion ring cluster.

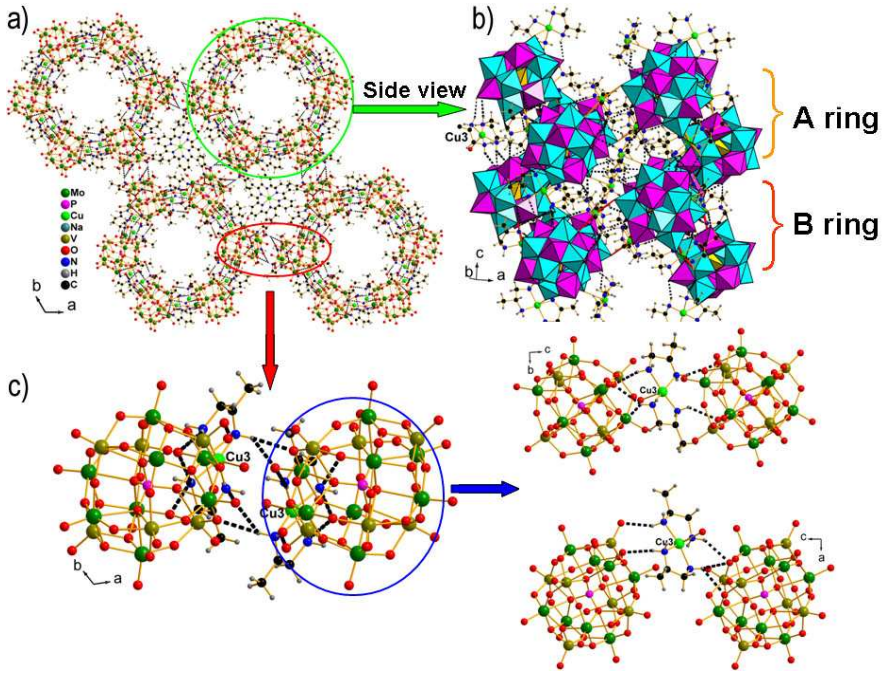

Figure S9 (a) Top view of the infinite 3-D architecture. (b) Side view of the ring cluster: A ring and B ring are linked together through the hydrogen-bonding interaction between the $[Cu(1)(1,2\text{-dap})_2]^{2+}$, $[Cu(2)(1,2\text{-dap})_2]^{2+}$, $[Cu(3)(1,2\text{-dap})_2(H_2O)]^{2+}$ cations and ring clusters. (c) In the *ab* plane, the neighbouring rings are linked together through the hydrogen-bonding interaction between the $[Cu(3)(1,2\text{-dap})_2(H_2O)]^{2+}$ cations and ring clusters; in the *bc* or *ac* plane, the hydrogen-bonding interaction also exist between the $[Cu(3)(1,2\text{-dap})_2(H_2O)]^{2+}$ cations and ring clusters.

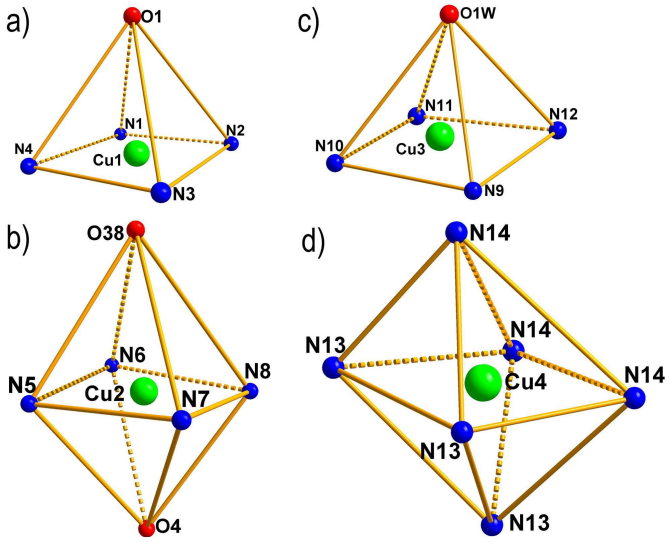

Figure S10 The coordination geometric frameworks of the $Cu(1)^{2+}$, $Cu(2)^{2+}$, $Cu(3)^{2+}$ and $Cu(4)^{2+}$ cations.

III. Physical measurement and characterization.

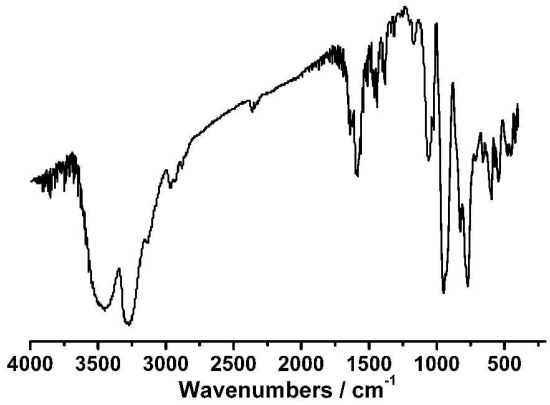

Figure S11. The IR spectrum of **1**.

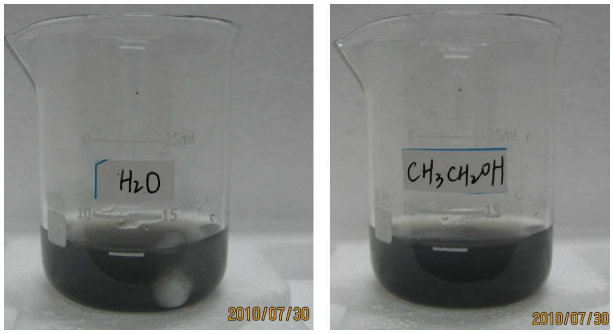

Figure S12. The photos for the solubility experiments of **1** in water (left) and ethanol solvent (right): 0.01 g sample **1** is added in the water or ethanol (10 mL). After stirred for 6 h, **1** still exist as the black solid in the solvent. Additionally, the solubility experiments phenomena in methanol and acetonitrile solvent is the same as above.

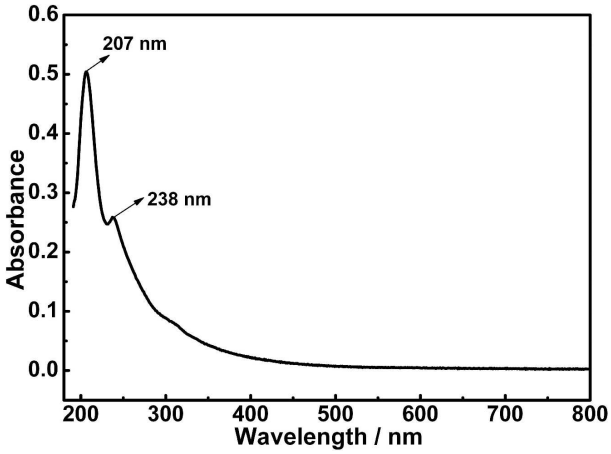

Figure S13. The UV spectrum of **1** in the saturated aqueous solution.

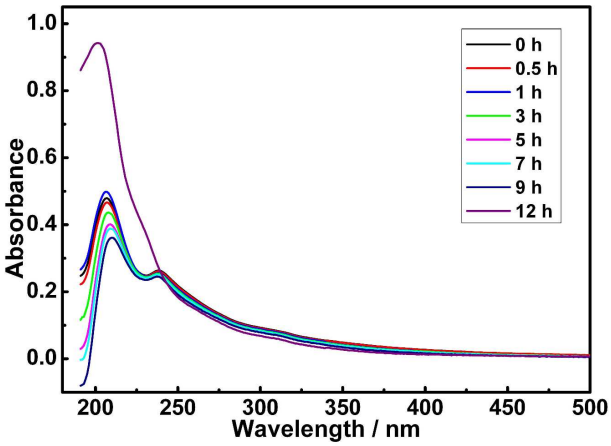

Figure S14. The in-situ UV spectra of **1** in the saturated aqueous solution with the period of 0–12 h, indicating that **1** begins to decompose after 9 h.

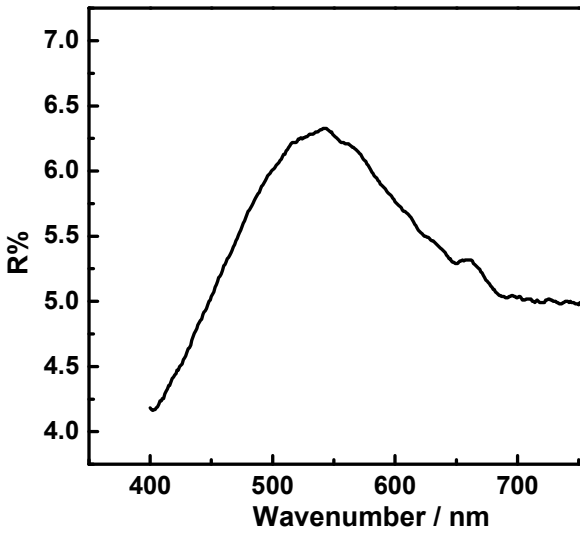

Figure S15. The visible-near-IR reflectance spectrum in solid of **1** showing an obvious absorption band at 544 nm attributed to the transition related to the black color.

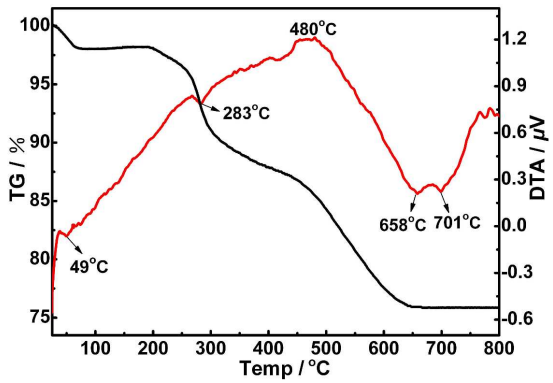

Figure S16. The TG-DTA curve of **1**.

Figure S17. The black crystals of **1**.

IV. Cationic exchange study.

Considering the 3-D supramolecular channel characteristic of **1** with $[Na(H_2O)]^+$ ions as the counter cations, we want to explore its cationic exchange property with other cations, such as Ag^+, NH_4^+, K^+ and Ba^{2+} ions.

Experiment: 0.01 g sample **1** was added to the 1 mol·L^{-1} $AgNO_3$, NH_4Cl, KCl and $BaCl_2$ aqueous solution, respectively. After the mixture was stirred for 6 h, the samples in $AgNO_3$, KCl and $BaCl_2$ aqueous solution still exist as the black solids (Figure S18 left, the sample in $AgNO_3$ as the example). The solids were filtered and washed with water. The results of the IR spectrum (Figure S19) and elemental analyses of the sample in $AgNO_3$ suggest that **1** does not show the obvious cationic exchange behavior with the Ag^+ cations. Similarly, **1** also does not show the obvious cationic exchange behavior with the K^+ or Ba^{2+} cations. Interestingly, when the sample was treated with NH_4Cl for 6 h, **1** was completely dissolved and decomposed (Figure S18 right, S20). We presume that **1** can't be stably in the acidic NH_4Cl aqueous solution due to the stronger acidity of the solution, which was further confirmed by the phenomenon that the sample was dissolved in 0.01 mol·L^{-1} HCl solution (Figure S21).

Figure S18. The cationic exchange experiments of **1** in 1 mol·L^{-1} $AgNO_3$ (left) and 1 mol·L^{-1} NH_4Cl aqueous solution (right).

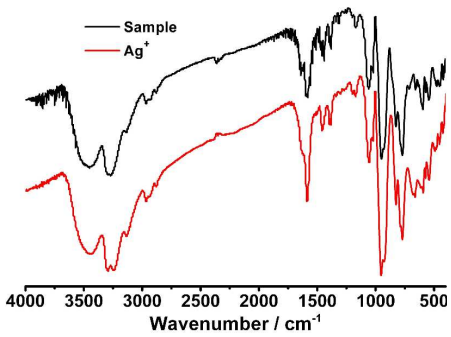

Figure S19. IR spectra of the original sample **1** and the sample treated by the 1 mol·L^{-1} $AgNO_3$.

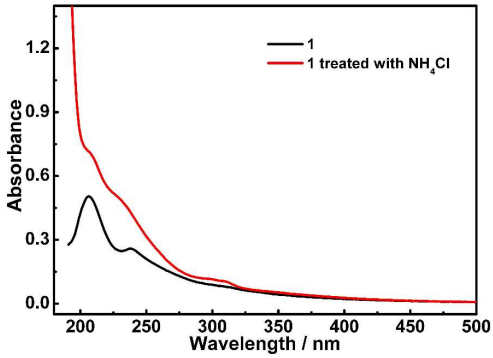

Figure S20. Comparison of the UV spectra of **1** and the sample treated by NH_4Cl solution.

Figure S21. The phenomenon that **1** was dissolved in 0.01 mol·L^{-1} HCl aqueous solution.

Table **S**1 Hydrogen Bond Lengths (Å) and Bond Angles (°) of **1**.

D–H···A	d(D–H)	d(H···A)	d(D···A)	□D–H···A
N1–H1C···O16	0.900	2.244	3.115	162.67
N1–H1D···O31	0.900	2.251	3.124	163.55
N2–H2B···O34	0.900	2.317	3.177	159.65
N2–H2C···O14	0.900	2.206	3.059	158.10
N3–H3D···O14	0.900	2.480	3.166	133.26
N3–H3D···O26	0.900	2.535	3.063	118.05
N3–H3E···O9	0.900	2.096	2.915	150.95
N4–H4B···O7	0.900	1.990	2.876	167.83
N4–H4C···O10	0.900	2.063	2.859	146.77
N5–H5A···O12	0.900	2.173	2.940	142.73
N5–H5B···O2	0.900	2.144	2.993	156.98
N6–H6D···O34	0.900	2.322	3.173	157.65
N6–H6D···O9	0.900	2.500	3.151	129.60
N6–H6E···O27	0.900	1.968	2.831	159.97
N7–H7C···O12	0.900	2.330	3.074	139.90
N7–H7C···O31	0.900	2.478	3.228	141.12
N8–H8A···O17	0.900	2.020	2.916	173.80
N8–H8B···O9	0.900	1.959	2.799	154.75
N9–H9D···O28	0.900	2.489	3.002	116.66
N9–H9D···O2	0.900	2.642	3.224	123.19
N9–H9E···O21	0.900	2.578	3.193	126.19
N9–H9E···O29	0.900	2.595	3.347	141.60
N10–H10C···O6	0.900	2.629	3.131	116.13
N10–H10C···O19	0.900	2.630	3.530	177.35
N10–H10D···O6	0.900	2.435	3.142	135.65
N11–H11B···O11	0.900	2.390	3.243	158.15
N11–H11C···O6	0.900	2.368	3.057	133.45
N11–H11C···O32	0.900	2.483	3.297	150.58
N12–H12D···O29	0.900	2.482	3.270	146.38